https://doi.org/10.5194/egusphere-2025-4822
Preprint. Discussion started: 20 October 2025

A mechanistic model of hypoxia-driven benthic carbon cycling integrating microbial energetics and faunal mortality

Kota Ishizuka[1] and Akio Sohma[1]

[1]Graduate School of Engineering, Osaka Metropolitan University, 3-3-138 Sugimoto, Sumiyoshi-ku, Osaka 558-8585, Japan

Corresponding author: Akio Sohma (sohma@omu.ac.jp)

https://doi.org/10.5194/egusphere-2025-4822
Preprint. Discussion started: 20 October 2025

Abstract. Hypoxia reduces the mineralization of organic detritus and increases mortality in benthic fauna, both of which alter carbon storage through complex changes in organic matter and calcium carbonate ($CaCO_3$) dynamics. To mechanistically assess these processes, we developed a new model that links oxic, suboxic, and anoxic mineralization pathways to microbial ATP production efficiency. This formulation was incorporated into the benthic–pelagic coupled model EMAGIN-B.C., resulting in an extended version designated EMAGIN-B.C.-MR (MR: mineralization rate). The model also includes revised mortality and metabolic suppression functions for benthic fauna under oxygen-deficient conditions and explicitly couples suspension-feeding benthos biomass with $CaCO_3$ production and burial fluxes. We applied EMAGIN-B.C.-MR to Tokyo Bay, a eutrophic coastal system prone to seasonal hypoxia, to simulate long-term changes in carbon cycling under hypoxic (0 mg L^{-1}) and non-hypoxic (5 mg L^{-1}) summer conditions. Results showed that hypoxia enhanced detritus storage and burial by both suppressing microbial degradation and reducing bioturbation and grazing due to suspension-feeding benthos mortality. Conversely, $CaCO_3$ production and burial declined owing to inhibited shell formation. These dynamics revealed that total carbon storage is shaped by interacting biogeochemical and ecological feedbacks, resulting in nonlinear trajectories under repeated hypoxic stress over decadal timescales. By integrating microbial energetics and oxygen-sensitive faunal responses, the EMAGIN-B.C.-MR model provides a mechanistic framework for assessing benthic carbon cycling under deoxygenation. This framework offers biogeochemical insights into the regulation of organic and inorganic carbon burial balance by oxygen availability – with implications for coastal carbon budgets, blue carbon management, and climate feedbacks – and is applicable to other oxygen-deficient environments such as eutrophic estuaries and semi-enclosed seas.

1 Introduction

According to the Sixth Assessment Report of the Intergovernmental Panel on Climate Change under the SSP5-8.5 scenario, the pathway projecting the highest temperature increase, the global average temperature is predicted to rise by up to 5.7 °C between 2081 and 2100 relative to the pre-industrial period (1850–1900) (IPCC, 2023). This highlights the urgency of reducing greenhouse gas emissions, particularly CO_2. The ocean, functioning as a major carbon sink, plays a pivotal role in mitigating climate change via carbon sequestration (Archer and Brovkin, 2008; Falkowski et al., 2000; IPCC, 2007; McLeod et al., 2011), which is governed by the following three primary mechanisms: (1) air–sea gas exchange of atmospheric CO_2 (carbon capture), (2) biological fixation of dissolved inorganic carbon via photosynthesis and calcification (carbon fixation), and (3) long-term burial of fixed carbon in sediments (carbon storage) (Sohma et al., 2018) (Fig. 1). Coastal areas, characterized by high

https://doi.org/10.5194/egusphere-2025-4822
Preprint. Discussion started: 20 October 2025

biological productivity, are particularly efficient in carbon capture, fixation (Nellemann et al., 2009), and storage, thereby identifying these areas as key regions for carbon cycle research (Alongi et al., 2016; Chen et al., 2013; Chmura et al., 2003; Donato et al., 2011; Fourqurean et al., 2012; Frankignoulle et al., 1998; Kubo and Kanda, 2017; Kuwae et al., 2016; Murdiyarso et al., 2015).

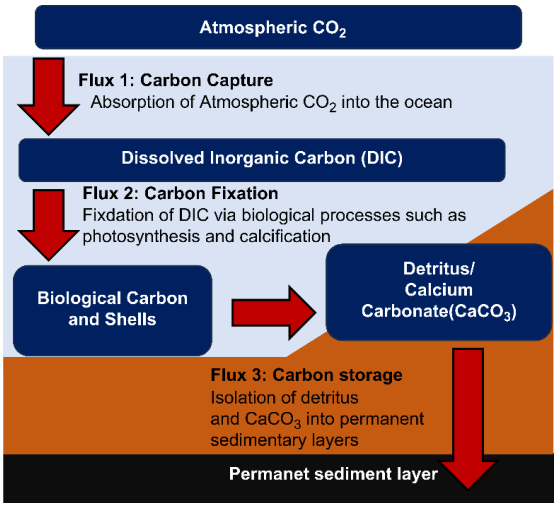

Figure 1. A schematic representation of climate change mitigation functions.

In enclosed coastal bays, such as Tokyo Bay, seasonal hypoxia in bottom waters has become an increasingly frequent occurrence during summer months (Breitburg et al., 2018; Diaz, 2001; Hanyu, 2020; Ishii and Ohata, 2010; Okubo et al., 2016; Rabalais et al., 2009). Hypoxia influences carbon storage via two major pathways. First, it suppresses aerobic mineralization, which promotes the preservation of organic matter (Andersen, 1996; Anderson et al., 1986; Bastviken et al., 2003; Benner et al., 1984; Blackburn, 1991; Canfield, 1989; Canfield, 1993; Canfield, 1994; Cowie et al., 1995; Emerson and Hedges, 1988; Fallon and Brock, 1979; Hansen and Blackburn, 1991; Rodger Harvey et al., 1995; Hedges, 1999; Hedges and Keil, 1995; Hollander et al., 1992; Hulthe et al., 1998; Ingall et al., 1993; Kristensen and Holmer, 2001; Kristensen and Holmer, 2001; Nguyen and Harvey, 1997; Paropkari et al., 1993; Sun et al., 1993; Sun et al., 1997; Wilson et al., 1985; Zsolnay, 1971). Second, it induces mortality in benthic fauna, which reduces dissolved inorganic carbon fixation via the food web originating from primary producers and the formation of shells (i.e., $CaCO_3$) by benthic fauna (Kristensen and Holmer, 2001; Rabalais et al., 2009). In this context, the storage of detritus due to suppressed oxic mineralization enhances carbon burial into permanent sedimentation layers (Burdige, 2007; Carey et al., 2018; Hartnett et al., 1998; Isidorova et al., 2019; Katsev and Crowe, 2015; LaRowe and Van Cappellen, 2011; Sobek et al., 2009), whereas the reduced production of benthic organisms and the decreased

https://doi.org/10.5194/egusphere-2025-4822
Preprint. Discussion started: 20 October 2025

deposition of $CaCO_3$ due to hypoxia-induced mortality act to lower it. In addition, the dissolution of $CaCO_3$ contributes to altering the alkalinity of seawater and pCO_2, thereby influencing the capacity of oceans to absorb atmospheric CO_2. Thus, the net effect of hypoxia on carbon storage is dependent on complex biogeochemical and ecological interactions.

Although the coastal ecosystem models developed to date, including EMAGIN-B.C., incorporate multiple redox pathways for organic matter mineralization, they often represent these processes using simplified first-order kinetics, without explicitly considering microbial energetic constraints (Aumont et al., 2003; Burdige, 2007; Carey et al., 2018; Cerco et al., 2006; Cowie et al., 1995; Fennel et al., 2011; Flynn, 2010; Hartnett et al., 1998; Hulthe et al., 1998; Isidorova et al., 2019; Katsev and Crowe, 2015; LaRowe and Van Cappellen, 2011; Meire et al., 2013; Reed et al., 2011; Sobek et al., 2009; Soetaert and Middelburg, 2009; Soetaert et al., 1996; Sohma et al., 2018; Stock et al., 2014; Wild-Allen et al., 2010; Yakushev et al., 2017; Yool et al., 2013). Moreover, although some models account for the oxygen-dependent mortality of benthic fauna (Butenschön et al., 2016; Nagao et al., 2005; Sohma et al., 2008), the interactions among mineralization efficiency, microbial growth, and faunal mortality under conditions of hypoxic stress remain poorly integrated.

In this study, we addressed these limitations by developing a novel model module that explicitly links redox-sensitive mineralization rates to microbial ATP production, grounded in microbial energetics and thermodynamics. Additionally, we refine hypoxia-induced mortality functions for benthic fauna based on threshold dissolved oxygen (DO) saturation levels derived from empirical observations. Our approach is novel given our representation of microbial responses to hypoxia as well as capturing the synergistic interplay between microbial metabolism and benthic faunal dynamics. These interactions determine the net carbon storage outcome in hypoxic sediments.

By integrating these advances into the established EMAGIN-B.C. benthic–pelagic coupled ecosystem model, we formulated an extended framework, designated as EMAGIN-B.C.-MR (mineralization rate), which can be applied to simulate biogeochemical feedback of hypoxia on benthic carbon storage. Our application of this model in Tokyo Bay enabled us to mechanistically analyze long-term changes in carbon burial and storage, thereby offering new insights into the role of hypoxia in coastal carbon dynamics.

2. Methods

In this study, we define “detritus storage” as the temporary accumulation of organic matter within the upper 10 cm of surface sediments, whereas “carbon burial” refers to the permanent sequestration of organic carbon within deeper sediment layers

https://doi.org/10.5194/egusphere-2025-4822
Preprint. Discussion started: 20 October 2025

beyond the active biogeochemical zone. To prevent ambiguity, we have intentionally avoided use of the term "detritus accumulation," which is replaced with either "storage" or "burial," depending on the context.

2.1 Modeling of mineralization

To quantify the effects of hypoxia on benthic carbon cycling, we extended the benthic–pelagic coupled ecosystem model EMAGIN-B.C. by incorporating a novel formulation of organic matter mineralization that explicitly accounts for microbial energetics (Zehnder and Stumm, 1988). The enhanced model, referred to as EMAGIN-B.C.-MR, simulates redox-sensitive mineralization rates based on adenosine triphosphoric acid (ATP) production efficiencies under oxic, suboxic, and anoxic conditions. This formulation draws on established microbial physiological principles and thermodynamic considerations, thereby enabling the mechanistic representation of energy-constrained microbial decomposition processes.

Although in numerous conventional ecosystem models, including EMAGIN-B.C., MEDUSA-2.0 (Yool et al., 2013), and BROM (Yakushev et al., 2017), mineralization is represented as a first-order function of detritus concentration, this approach neglects important redox-dependent constraints on microbial growth and metabolism. Our approach introduces microbial ATP production rates and biomass dynamics as key mediators of organic matter degradation, thereby contributing to more realistic simulations of mineralization processes under conditions of hypoxic stress.

To capture the variation in microbial growth rates under different redox conditions (oxic > suboxic > anoxic) and to incorporate pathway-specific differences in mineralization efficiency, we made the following assumptions:

The rate of detritus mineralization ($M_{DET}\ T^{-1}$) by microorganisms is proportional to the amount of detritus ($M_{DET}\ T^{-1}$).

The rate of detritus mineralization ($M_{DET}\ T^{-1}$) by microorganisms is proportional to microbial biomass (M_{BAC}).

The rate of microbial growth ($M_{BAC}\ T^{-1}$) is proportional to microbial biomass (M_{BAC}).

The rate of ATP acquisition ($M_{ATP}\ T^{-1}$) from mineralization by microorganisms is proportional to the rate of microbial mineralization ($M_{DET}\ T^{-1}$).

The rate of ATP generation ($M_{ATP}\ T^{-1}$) by microorganisms is proportional to the rate of Gibbs free energy production associated with their respective respiratory reactions.

The rate of microbial growth ($M_{BAC}\ T^{-1}$) is proportional to the rate of ATP acquisition ($M_{ATP}\ T^{-1}$)

(Here, M means carbon mass, T means time)

https://doi.org/10.5194/egusphere-2025-4822
Preprint. Discussion started: 20 October 2025

Under these assumptions, we formulated the rate of detritus mineralization (Table 1 and Fig. 2). This formulation introduces the following three parameters:

1. ATP acquisition per unit organic matter mineralized (α_{ATP}):

$\alpha_{ATP}[\mathrm{M_{ATP}\ M_{DET}}^{-1}]$ represents the molar concentration of ATP (M_{ATP}) generated per unit of organic matter (detritus, $\mathrm{M_{DET}}$) mineralized. Compared with anaerobic microorganisms, this value is greater for oxic (aerobic) microbes, reflecting the higher energy acquisition efficiency of the latter and the more rapid rate of oxic mineralization compared with anoxic processes. The value of α_{ATP} for each class of microorganism was estimated based on the Gibbs free energy (δ_{ene}) (Canfield et al., 2005) generated during each type of mineralization (oxic and anoxic), the energy consumed by microorganisms during ATP generation (ε_{ATP}) (Bailey and Ollis, 1986) and the proportion of energy available for ATP generation (β_{ATP}) from mineralization energy (Payne, 1970).

2. Microbial biomass per ATP generated (Y_{ATP}):

$Y_{ATP}[\,M_{BAC}\ M_{ATP}{}^{-1}]$ represents the proliferation of bacterial biomass per mole of ATP generated, the value of which is assumed to be constant in different classes of microorganism (oxic and anoxic), as previously indicated (Jin, 2012).

3. Ratio of the rate of detritus consumption to the rate of microbial growth (R):

$R[M_{DET}T^{-1}/M_{BAC}T^{-1}]$ is treated as a tuning parameter that represents the ratio between the rates at which detritus is consumed and microbial biomass grows.

By incorporating these three parameters as multiplicative factors into the organic matter mineralization rate equation of existing models, we developed a detritus mineralization rate equation for EMAGIN-B.C.-MR.

Consequently, EMAGIN-B.C.-MR facilitated a more realistic evaluation of the reduction in detritus mineralization rates under hypoxic conditions and the corresponding increase in carbon burial.

Table 1. Model formulation for the rate of detritus mineralization in EMAGIN-B.C.-MR

$\mathrm{Ddet}(i, j) = \alpha_{ATP}(j) \times Y_{ATP} \times R(j) \times \alpha(i) \times g(j) \times f(T, i) \times \mathrm{DET}(i)$

where i = 1 : Labile detritus, i = 2 : Quasi labile detritus, i = 3 : Refractory detritus

j = 1: Oxic mineralization (oxygen consumption), j = 2: Suboxic mineralization (nitrate consumption), j = 3: Anoxic mineralization (iron, manganese, and sulfate consumption)

Symbol	Description	Unit	Value	Reference

https://doi.org/10.5194/egusphere-2025-4822
Preprint. Discussion started: 20 October 2025

$\alpha_{ATP}(j)$	ATP energy required for the decomposition of detritus per unit mass. ※$\alpha_{ATP}(j) = \sigma_{ene}(j)/\beta_{ATP} \times \varepsilon_{ATP}$	$M_{ATP}\ M_{DET}^{-1}$	cal	-
$\sigma_{ene}(j = 1)$	The amount of energy obtained via oxic (aerobic) respiration	$kJ_{ENE}\ M_{DET}^{-1}$	402	(Zehnder and Svensson, 1986)
$\sigma_{ene}(j = 2)$	The amount of energy obtained via suboxic respiration	$kJ_{ENE}\ M_{DET}^{-1}$	359	(Zehnder and Svensson, 1986)
$\sigma_{ene}(j = 3)$	The amount of energy obtained via anoxic (anaerobic) respiration	$kJ_{ENE}\ M_{DET}^{-1}$	223	(Zehnder and Svensson, 1986)
ε_{ATP}	The proportion of σ_{ene} used for ATP synthesis	$kJ_{ATP}\ M_{ATP}^{-1}$	0.4	(Fenchel and Finlay, 1995)
β_{ATP}	The amount of energy required to synthesize one molecule of ATP	$kJ_{ATP}\ kJ_{ENE}^{-1}$	30.88	(Russell and Cook, 1995)
Y_{ATP}	Microbial growth per unit of ATP	$M_{BAC}mol_{ATP}^{-1}$	5	(Canfield et al., 2005)
R(j = 1)	The rate of organic matter consumption per unit of oxic (aerobic) microbial growth rate	$M_{DET}\ M_{BAC}^{-1}$	cal	tuning
R(j = 2)	The rate of organic matter consumption per unit of suboxic microbial growth rate	$M_{DET}\ M_{BAC}^{-1}$	cal	tuning
R(j = 3)	The rate of organic matter consumption per unit of anaerobic (anoxic) microbial growth rate	$M_{DET}\ M_{BAC}^{-1}$	cal	tuning
α(i)	Rate constant	T^{-1}	-	(Sohma et al., 2018)
g(i)	Oxygen–nitrate concentration-dependent function	-	-	(Sohma et al., 2018)
f (T, i)	Water temperature-dependent function	-	-	(Sohma et al., 2018)

https://doi.org/10.5194/egusphere-2025-4822
Preprint. Discussion started: 20 October 2025

DET(i)	Amount of detritus (organic matter) storage	$M_{DET}\ L^{-3}$	-	(Sohma et al., 2018)

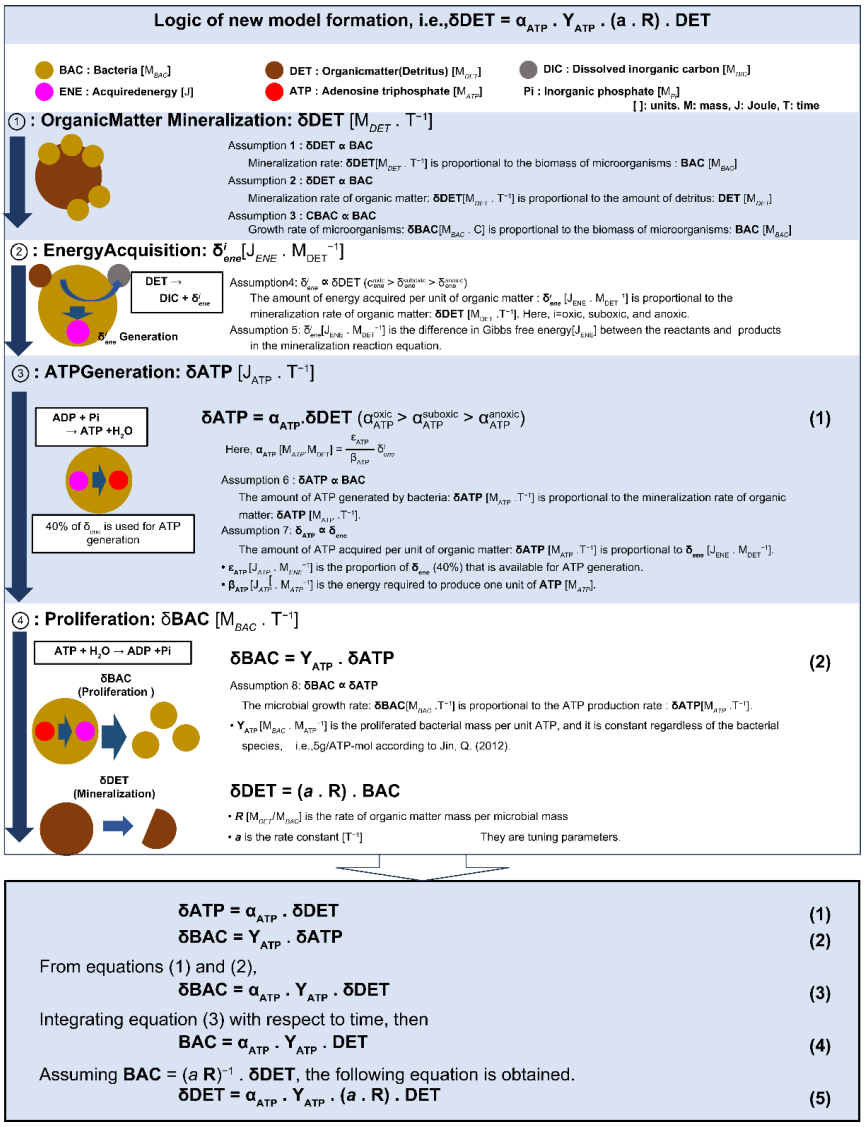

Figure 2. Logic of the new modeling of mineralization.

https://doi.org/10.5194/egusphere-2025-4822
Preprint. Discussion started: 20 October 2025

2.2 Modeling of hypoxia tolerance for benthic fauna

When using both EMAGIN-B.C. and EMAGIN-B.C.-MR models, two types of benthic fauna are considered, namely, suspension (SFB) and deposit (DFB) feeding benthos, the mortality of which due to hypoxia is represented using the functions of temperature and DO concentrations (Table 2).

Compared with the EMAGIN-B.C. model, the primary enhancement of EMAGIN-B.C.-MR lies in the re-definition of the values of parameters deDO51 and deDO52, which represent the DO saturation thresholds (based on 24 h averages) for hypoxia tolerance. These threshold values were set in the range from 0.30 to 0.75 based on fisheries laboratory reports [Hypoxia Information of Ise and Mikawa Bay (R5-11), https://www.pref.aichi.jp/uploaded/attachment/472338.pdf], previous modeling studies (Sasaki et al., 2009), and laboratory experiments that examined hypoxia tolerance in benthic organisms (Shimo et al., 2004).

Here, the DO thresholds for benthic invertebrates are defined in terms of percent oxygen saturation, following standard practice in experimental studies (e.g., Diaz and Rosenberg, 1995; Gray et al., 2002). In the model, DO saturation (DO_sat) is dynamically calculated at each time step based on water temperature using empirical solubility functions (e.g., Garcia and Gordon, 1992). Percent saturation is then computed as the ratio of actual DO concentration to DO_sat. This method facilitates ecologically meaningful and temperature-consistent threshold application across time and space. Thus, even when DO concentrations (mg L^{-1}) are input, they are internally converted to percent saturation to determine benthic faunal responses.

Table 2. Hypoxia tolerance equations for benthic fauna in EMAGIN-B.C.-MR

Mortality of SFB (suspension feeders): $Dsfb4 = -v511 \times u512 \times SFB$
Mortality of DFB (deposit feeders): $Ddfb4 = -v521 \times u522 \times DFB$
v511: Temperature-dependent function for SFB mortality
u512: Dissolved oxygen (DO) concentration-dependent function for SFB mortality
v521: Temperature-dependent function for DFB mortality
u522: DO concentration-dependent function for DFB mortality
SFB: Biomass of suspension feeders
DFB: Biomass of deposit feeders

https://doi.org/10.5194/egusphere-2025-4822
Preprint. Discussion started: 20 October 2025

$u512 = Ade511 + Ade512 \times [1- min(1.0, dorat/deDO51)]$	
$u522 = Ade521 + Ade522 \times [1- min(1.0, dorat/deDO52)]$	
dorat: 24-h average value of oxygen saturation	
Ade511: Background mortality rate of SFB at 0 °C (applies at all DO levels)	
Ade512: Hypoxia-induced incremental mortality rate of SFB at 0 °C (zero when dorat ≥ deDO51	
deDO51: Oxygen saturation threshold causing hypoxia for SFB	
Ade521: Background mortality rate of DFB at 0 °C (applies at all DO levels)	
Ade522: Hypoxia-induced incremental mortality rate of DFB at 0 °C (zero when dorat ≥ deDO52dorat)	
deDO52: Oxygen saturation threshold causing hypoxia for DFB	

Note. *Ade511* (*Ade521*) is background mortality; *Ade512* (*Ade522*) is the hypoxia-induced increment that vanishes at or above the DO-saturation threshold *deDO51*(deDO52).

3. Application of the model: construction of the Base Case

To evaluate the effects of hypoxia on carbon storage, we applied the extended model "EMAGIN-B.C.-MR," which incorporates oxygen-dependent mineralization processes and revised hypoxia tolerance of benthic fauna, to Tokyo Bay. The objectives of the application were to: (1) verify the model's validity, and (2) construct a calculation scenario (Base Case) for comparison with two analytical scenarios (Cases 1 and 2). The Base Case was designed to reproduce the representative seasonal dynamics of the Tokyo Bay ecosystem around the year 2000 (1998 to 2002), for which abundant observational data are available for both pelagic and benthic systems. The model's validity was assessed by comparing the simulation results of the Base Case with the observations during this period.

3.1. Geomorphological and temporal settings

In the model configuration, Tokyo Bay was divided into 26 horizontal segments. The pelagic system (water column) was vertically divided into 2 m intervals. The benthic system (sediment layer) was divided into 30 vertical layers covering the upper 10 cm, with thinner layers closer to the sediment surface (Fig. 3). The surface layers of the benthic system were represented with millimeter-scale resolution to resolve sharp gradients associated with oxic, suboxic, and anoxic mineralization. The time resolution was set to 0.2 h to capture both diurnal and seasonal variations.

https://doi.org/10.5194/egusphere-2025-4822
Preprint. Discussion started: 20 October 2025

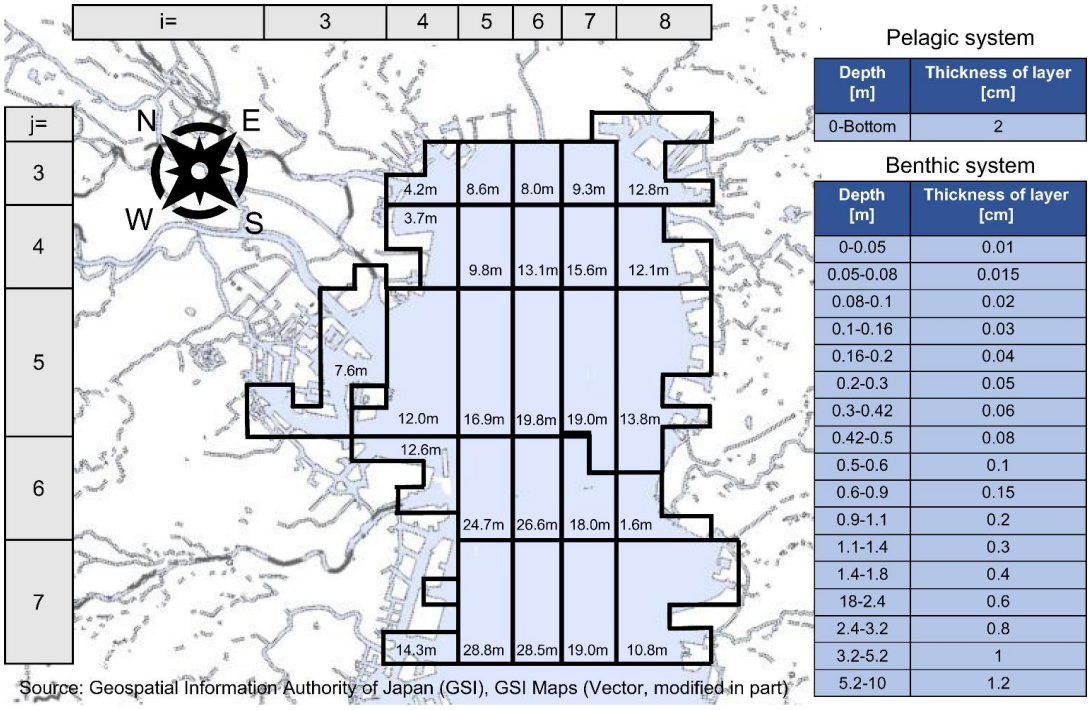

Figure 3. Calculation domain of EMAGIN-B.C.-MR (area: 728 km²). Left: grid coordinates (i, j) and water depth. Right: vertical layer thickness.

3.2. Boundary conditions, initial values, and biogeochemical parameters

EMAGIN-B.C.-MR is an extension of EMAGIN-B.C. (Sohma et al., 2018) and ECOHYM (Sohma et al., 2008). Therefore, the following components are shared among the three models: (1) model variables (model components) across pelagic and benthic systems (e.g., phytoplankton [PP], zooplankton, benthic microalgae, benthic invertebrates [suspension and deposit feeders], fast-/slow-/refractory detritus, dissolved organic matter, NH_4-N, NO_3-N, PO_4-P, DO, reduced substances [total of SO_4^{2-}, Mn^{4+}, and Fe^{3+}], dissolved inorganic carbon, total alkalinity, pH, and pCO_2); (2) driving forces (e.g., river discharge, nutrient loading, solar radiation, wind speed, tidal height, temperature, salinity, and boundary values of model variables); (3) initial values of model components; and (4) biogeochemical parameters (except for those specifically related to oxygen-dependent mineralization and hypoxia tolerance of benthic fauna).

In the Base Case, the boundary conditions, initial values, and biogeochemical parameters, excluding those related to oxygen-dependent mineralization and hypoxia tolerance of benthic fauna, were set identically to those used in previous applications of EMAGIN-B.C. to Tokyo Bay (Sohma et al., 2008, 2018). Specifically, the boundary conditions were constructed as annual

https://doi.org/10.5194/egusphere-2025-4822
Preprint. Discussion started: 20 October 2025

cyclic functions based on observational data from 1998 to 2002, facilitating the reproduction and simultaneous simulation of seasonal variations that are representative of the Tokyo Bay ecosystem around the year 2000. Initial values were set to the estimated average values on April 1st based on data from 1998 to 2002.

3.3. Execution and interpretation of the Base Case

Using the above settings, the EMAGIN-B.C.-MR model was run until all model variables reached an annual periodic steady state, where seasonal and diurnal variations are repeated each year. Approximately 20 years of simulation were required to reach this state, which corresponds to the time needed for organic particles settling from the pelagic layer to be buried to a depth of 10 cm in the sediment. The resulting Base Case thus represents the steady-state ecosystem of Tokyo Bay under conditions in which the forcing functions (boundary conditions) characteristic of around the year 2000 were applied repeatedly for 20 years. A more realistic reconstruction of ecosystem dynamics around the year 2000 would ideally involve setting the model's initial conditions to values from 1980 and defining the temporal changes in boundary conditions from 1980 to 2000. However, such datasets are not currently available. Moreover, seasonal patterns from 1998 to 2002 showed little interannual variability. Therefore, the Base Case was considered to be a representative approximation of the seasonal dynamics in Tokyo Bay around the year 2000.

4. Model validation: assessment using the Base Case

To evaluate the performance of EMAGIN-B.C.-MR, we compared its output with observed values for key ecological variables from 1998 to 2002. Specifically, we compared DO, particulate organic carbon (POC), PP, nitrate (NO_3), ammonium (NH_4), and phosphate (PO_4) (Table 3 and Fig. 4). We determined the correlation coefficient (R), root mean square error (RMSE), and P-value for different depths and time points (Table 3). Observational data were obtained from representative stations in Tokyo Bay between 1999 and 2002.

The results indicate that the model can successfully reproduce the seasonal reduction in bottom-layer DO and trends in POC. A representative comparison is highlighted at grid point (i, j) = (6, 4) (Fig. 4), indicating the model's ability to capture seasonal hypoxia in the bottom layer, with an R of 0.83 and an RMSE of 1.64 mg L^{-1}.

Overall, the modeled outputs for DO, POC, PP, NO_3, NH_4, and PO_4 reflect the integrated effects of biological, chemical, and physical processes across the pelagic–benthic system. This confirms that EMAGIN-B.C.-MR meets the necessary conditions

https://doi.org/10.5194/egusphere-2025-4822
Preprint. Discussion started: 20 October 2025

for realistically representing the Tokyo Bay ecosystem, supporting its application to mechanistic analysis of hypoxia-driven carbon dynamics.

Table 3. Analysis of correlation coefficients (R) and root mean square errors (RMSE) between observed and calculated values in EMAGIN-B.C.-MR

Item	Water depth	Correlation coefficient (R)	RMSE	Observed averaged value	P-value	Number of data points
DO	Surface layer	0.47	1.96	8.85	$P < 0.01$	232
	Bottom layer	0.83	1.64	5.43	$P < 0.01$	232
NO_3	Surface layer	0.73	0.22	0.41	$P < 0.01$	232
	Bottom layer	0.60	0.14	0.27	$P < 0.01$	232
NH_4	Surface layer	0.59	0.25	0.34	$P < 0.01$	232
PO_4	Surface layer	0.66	0.03	0.05	$P < 0.01$	232
	Bottom layer	0.51	0.03	0.05	$P < 0.01$	232
PP	Surface layer	0.46	0.93	0.76	$P < 0.01$	232
POC	Surface layer	0.80	0.81	2.99	$P < 0.01$	100
	Bottom layer	0.41	0.59	1.85	$P < 0.01$	78

https://doi.org/10.5194/egusphere-2025-4822
Preprint. Discussion started: 20 October 2025

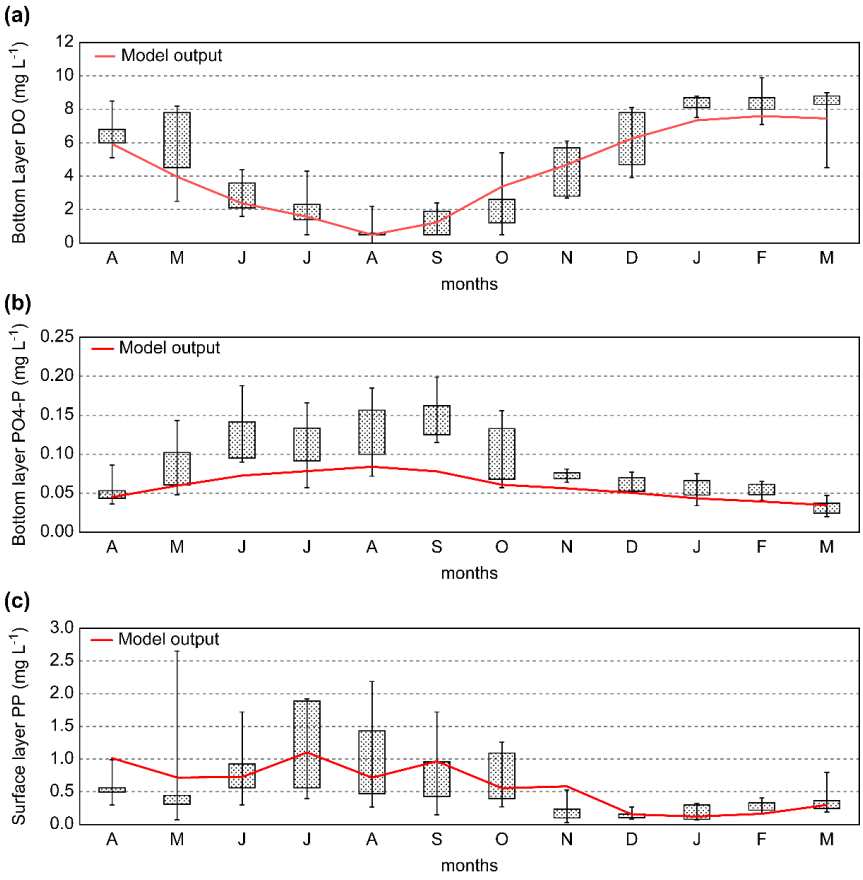

Figure 4. Comparison of calculated (model output) and observational data [region (i, j) = (6, 5) in Figure 3]. a. Comparison of dissolved oxygen (DO) concentrations in the bottom layer. b. Comparison of phytoplankton (PP) in the surface layer. c. comparison of PO_4-P in the bottom layer.

5. Sensitivity analysis

To evaluate the long-term effects of summer hypoxia using EMAGIN-B.C.-MR, we conducted a sensitivity analysis based on the verified Base Case. Specifically, two scenarios were defined in which bottom-layer DO in the pelagic system was forcibly set to 0 mg L^{-1} (Case 1: hypoxic) and 5 mg L^{-1} (Case 2: non-hypoxic) for 31 days from August 1st to 31st each year (Table 4, Fig. 5).

Both scenarios were initialized using April 1st values from the Base Case steady state, and simulations were run for 100 years. During each August, the bottom-layer DO was overwritten to 0 mg L^{-1} or 5 mg L^{-1} depending on the scenario, whereas all other conditions, including DO, except during August, remained consistent with the Base Case. These scenarios thus represent

https://doi.org/10.5194/egusphere-2025-4822
Preprint. Discussion started: 20 October 2025

hypothetical systems in which Tokyo Bay undergoes annual, recurring hypoxic, or non-hypoxic conditions every August for a century.

These scenarios were not intended to reproduce specific years but rather to represent extreme end-member conditions (0 and 5 mg L^{-1}) to evaluate the long-term sensitivity of benthic carbon dynamics to oxygen availability. In this context, Case 1 (0 mg L^{-1}) and Case 2 (5 mg L^{-1}) were designed as contrasting end-member cases, not as realistic representations of summer DO conditions, to isolate and clarify the mechanistic impacts of oxygen availability on benthic ecosystems and carbon cycling.

In both scenarios, the Banzu tidal flat (i, j = 8, 6) was maintained at 5 mg L^{-1} throughout the 100-year simulation, as this area is considered unlikely to become hypoxic. This setting ensured a continuous supply of benthic invertebrate larvae from Banzu to other parts of the bay, even under the prolonged hypoxic conditions in Case 1. For both scenarios, annual average values were extracted for simulation Years 1, 10, 30, and 100, and the time-series results were compared among Case 1, Case 2, and the Base Case to quantify the effects of hypoxia on carbon storage. The Base Case had already reached an annual steady state; therefore, the annual averages for Years 1, 10, 30, and 100 were identical to those at Year 0. This serves as the reference in subsequent figures.

Table 4. Sensitivity analysis scenarios

Analysis scenario	Dissolved oxygen (DO) concentration in the bottom waters in August
Base Case	Average annual variation from 1999 to 2002
Case 1: When the bottom waters become anoxic during the summer (hypoxic conditions)	DO = 0 mg L^{-1}
Case 2: When the bottom waters do not become anoxic during the summer (non-hypoxic conditions)	DO = 5 mg L^{-1}

https://doi.org/10.5194/egusphere-2025-4822
Preprint. Discussion started: 20 October 2025

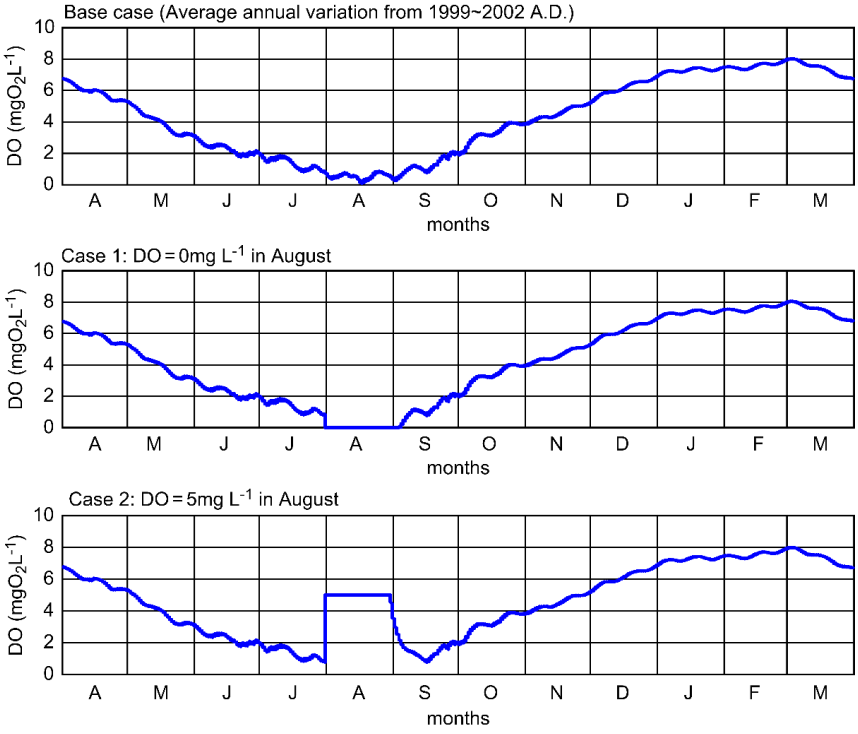

Figure 5. Time series of analysis scenarios, showing dissolved oxygen (DO) concentrations within the bottom layers of the pelagic system. Example: (i, j) = (6, 5).

6 Results and discussion

6.1 Long-term changes in carbon storage function

Figure 6 shows the year-on-year changes in the carbon storage function across the entire calculation domain of Tokyo Bay (728 km², shown in Fig. 3). The figure presents the annual average values for the rate at which carbon moves from a sediment depth of 10 cm to deeper layers (Carbon storage, Flux3 in Fig. 1, M T^{-1}), and the amount of carbon stored within the sediment layer from 0 to 10 cm depth (t C).

https://doi.org/10.5194/egusphere-2025-4822
Preprint. Discussion started: 20 October 2025

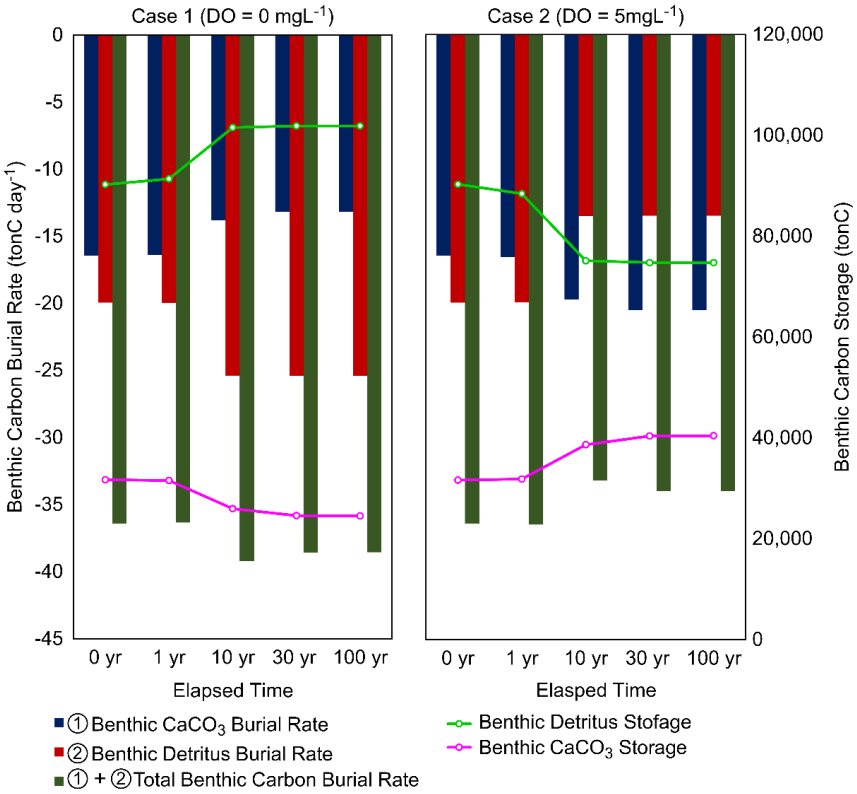

Figure 6. Time-series of changes in detritus storage and burial rates in the benthic system. Burial rate (Flux 3 in Figure 1) represents the annual average total value across the entire bottom layer of the benthic system (the square of the entire bottom layer = 728 km², Figure 3). The amount of stored carbon indicates the annual average total value across the entire benthic system (the volume of the entire benthic system = 728 km² × 10 cm depth). Positive rates represent processes that contribute to an increase in detritus storage, whereas negative rates represent processes that lead to a decline. Note: Base Case values remain constant over time and are therefore not shown separately.

Compared with the Base Case (i.e., the values at 0 yr, since the Base Case remained unchanged over time), the results revealed that under Case 1 (hypoxic conditions), the amount of stored detritus in the benthic system increased over time, whereas there were reductions in the storage of $CaCO_3$. Similarly, the rate at which detritus was buried showed an increasing trend over time, whereas the rate of benthic $CaCO_3$ burial declined. The total benthic burial rate, which is the sum of the benthic detritus and benthic $CaCO_3$ burial rates, peaked in Year 10 and subsequently declined in Years 30 and 100.

For Case 2 (non-hypoxic conditions), we detected trends that were the opposite to those observed in Case 1, thereby indicating that hypoxic conditions enhance the rates of benthic detritus storage and burial, whilst simultaneously reducing the rates of benthic $CaCO_3$ storage and burial, with these effects becoming more pronounced over time.

https://doi.org/10.5194/egusphere-2025-4822
Preprint. Discussion started: 20 October 2025

6.2. Mechanistic analysis of benthic detritus dynamics

To elucidate the influence of changes in bottom-water DO concentrations on the detrital carbon burial flux at a sediment depth of 10 cm (Flux 3 in Fig. 1, M T^{-1}) and on the amount of detritus stored in the benthic system to the same depth (M), we conducted a mechanistic analysis of detritus production and consumption processes.

Figure 7 illustrates a conceptual diagram of the production and consumption pathways of benthic detritus, whereas Fig. 8 presents time-series changes in the annual average rates of production and consumption over the entire Tokyo Bay domain. Differences between Case 1 (hypoxic condition) and Case 2 (non-hypoxic condition) are shown in Fig. 9. The correspondence between each bar chart item and the respective ecosystem processes is also indicated in Fig. 7.

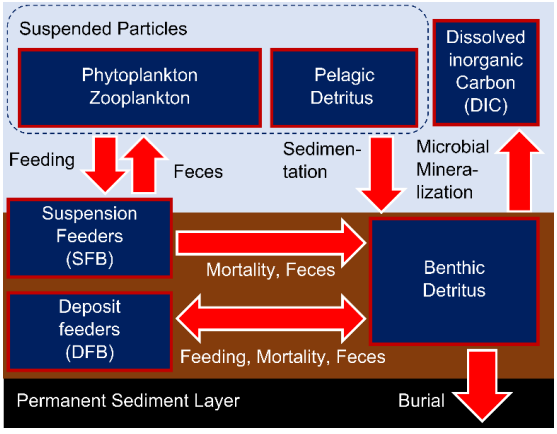

Figure 7. A conceptual diagram illustrating the mechanisms associated with detritus production and consumption in the benthic system.

https://doi.org/10.5194/egusphere-2025-4822
Preprint. Discussion started: 20 October 2025

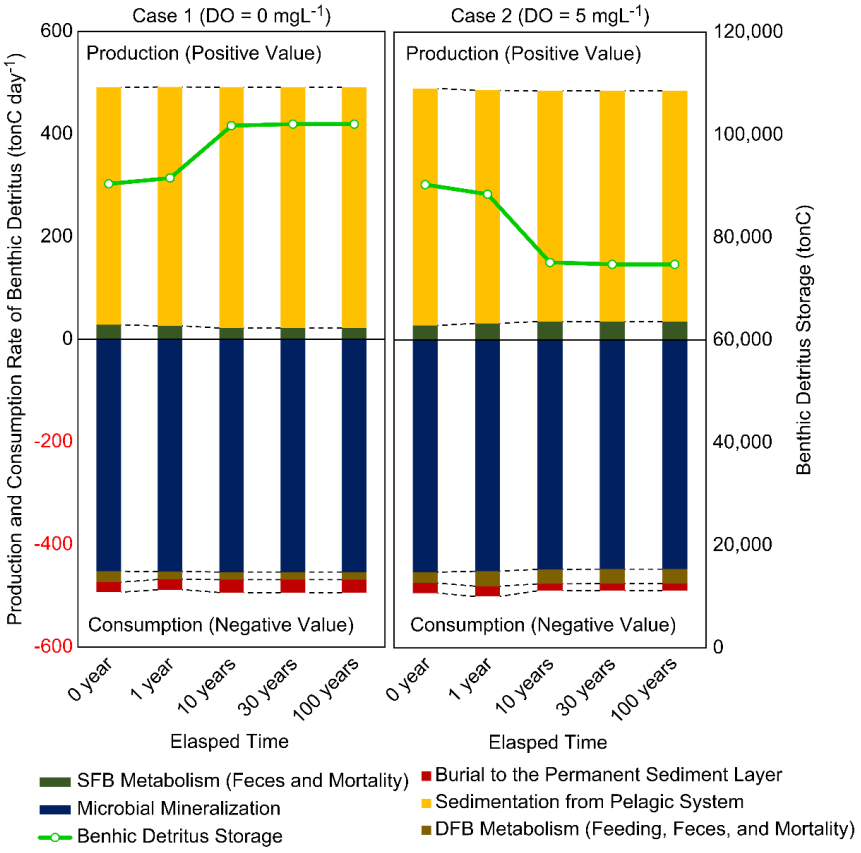

Figure 8. Annual average rates of benthic detritus production and consumption. Total values across the entire benthic system (728 km² × 10 cm) (positive for production and negative for consumption). Note: Base Case values remain constant over time and are therefore not shown separately.

https://doi.org/10.5194/egusphere-2025-4822
Preprint. Discussion started: 20 October 2025

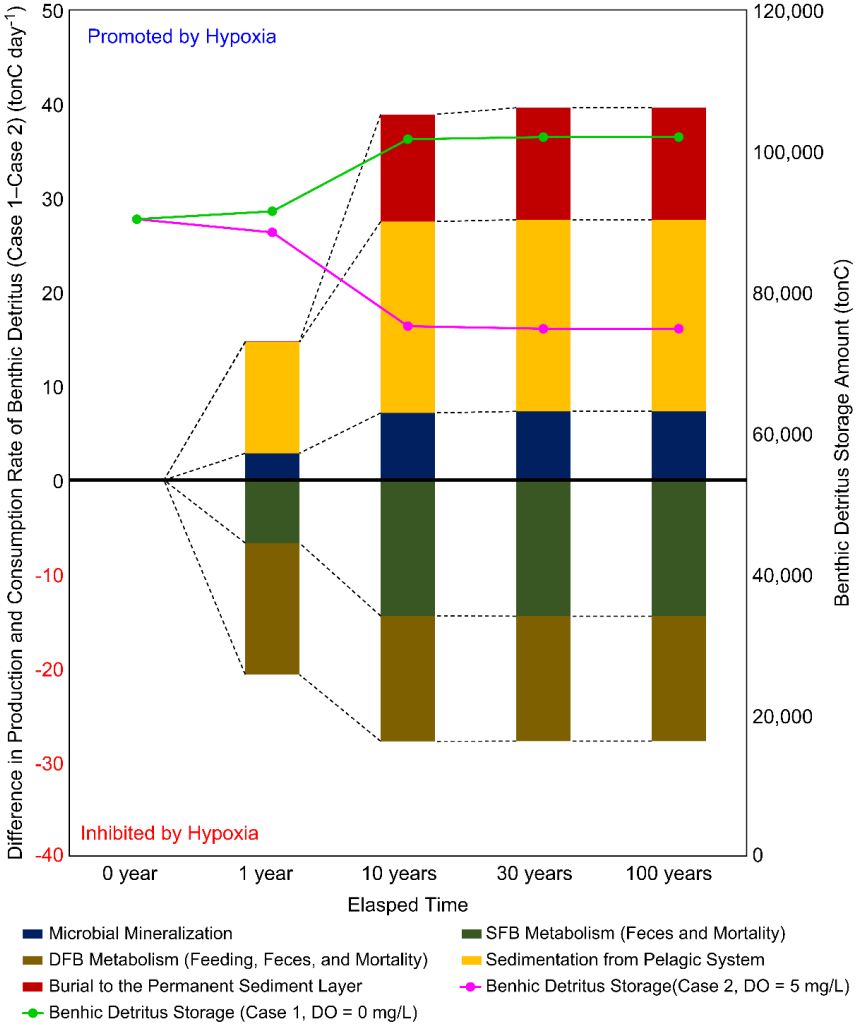

Figure 9. Differences in annual average rates of benthic detritus production and consumption between the Case 1 and Case 2 scenarios (Case 1 − Case 2). Total values across the entire benthic system (728 km² × 10 cm) (positive for production and negative for consumption).

Figure 8 illustrates annual average rates of benthic detritus production and consumption. As noted above, because the Base Case had already reached an annual steady state, the values at Year 0 serve as a constant reference over time. As shown in Fig. 8, the production of benthic detritus is primarily driven by organic matter sedimentation from the pelagic system, whereas consumption is largely governed by microbial mineralization. Biological processes involving SFB and DFB – such as feeding, feces, and mortality – also contribute to detritus production and consumption, but their overall influence is smaller compared to sedimentation and mineralization.

https://doi.org/10.5194/egusphere-2025-4822
Preprint. Discussion started: 20 October 2025

Figure 9 illustrates the differences in annual average rates of benthic detritus production and consumption between the Case 1 and Case 2 scenarios (Case 1 − Case 2). The comparison between two cases reveals that, under hypoxic conditions (Case 1), detritus production associated with fecal pellet formation and mortality by SFB and DFB (M T^{-1}) was lower than under non-hypoxic conditions (Case 2). This reduction is attributable to mass mortality of benthic fauna caused by hypoxia. In contrast, detritus sedimentation from the pelagic layer, mineralization within sediments, and the burial flux of organic matter at a sediment depth of 10 cm (Flux 3 in Fig. 1) all increased under hypoxic conditions.

The increase in detritus sedimentation from the pelagic layer (M T^{-1}) is attributed to reduced grazing pressure due to a decline in SFB populations, which led to an accumulation of suspended organic matter in the water column and, consequently, enhanced sedimentation, as well as decreased mineralization efficiency in the pelagic zone under low-oxygen conditions. The increase in mineralization flux within sediments (M T^{-1}) was driven by a decrease in the mineralization rate per unit detritus (T^{-1}) under hypoxia, which was offset by an increase in the detritus mass (M) accumulated in the sediment. This seemingly paradoxical outcome – an increased mineralization flux despite a reduced mineralization rate – is explained by the accumulation of detritus in hypoxic sediments. The elevated detritus mass effectively compensates for the reduced per-unit rate, resulting in a net increase in total flux. This relationship is illustrated in Fig. 9, where both individual rate components and total fluxes are compared between Case 1 and Case 2.

As a result, the total mineralization flux, defined as mineralization flux = mineralization rate × detritus mass (M T^{-1}), was greater under Case 1 than Case 2.

Furthermore, the combined metabolic changes in microbial and benthic faunal communities under hypoxic conditions enhanced the accumulation of benthic organic matter, leading to an increased burial flux into deeper sediments.

These complex mechanisms underlying the hypoxia-induced changes in benthic organic matter storage and burial were made quantifiable for the first time through the integration of an ATP-based microbial metabolic model and a physiological model of benthic faunal activity. This integrated modeling approach represents a key novelty and scientific contribution of the present study.

Figure 10 shows the long-term changes in the rate of mineralization per unit detritus (T^{-1}) and detritus storage in the benthic system (sediment depth of 10 cm) at grid point (i, j) = (6, 5). Over the 100-year simulation period, the rate of mineralization per unit detritus was consistently lower in Case 1 (August bottom water DO = 0 mg L^{-1}, representing hypoxic conditions) than in Case 2 (August bottom water DO = 5 mg L^{-1}, representing non-hypoxic conditions).

https://doi.org/10.5194/egusphere-2025-4822
Preprint. Discussion started: 20 October 2025

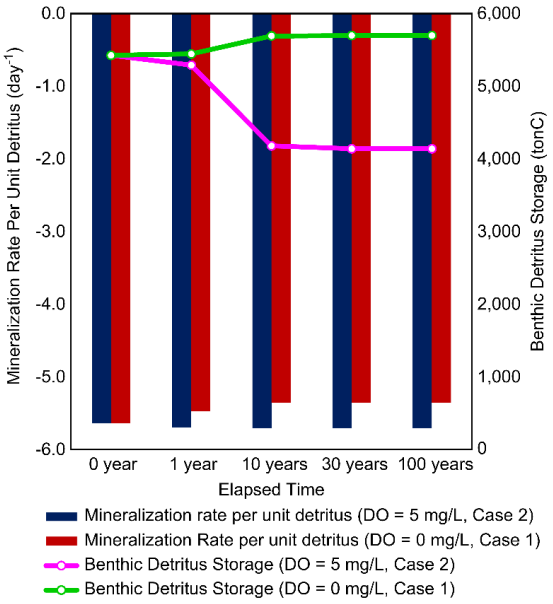

Figure 10. The rates of mineralization per unit weight of benthic detritus. Benthic Detritus Storage Amount represent total value values of benthic system at (i, j) = (6, 5) (40 km² × 10 cm).

In Case 1, detritus storage was characterized by a slight increase from Year 1 to Year 10, followed by a more gradual rise thereafter. In contrast, in Case 2, detritus storage underwent a significant decline from Year 1 to Year 10, with a slower rate of decline thereafter. These results indicate that a reduction in the rate of mineralization per unit detritus promotes an increase in detritus storage, whereas an increase in mineralization rates results in a reduction in detritus storage.

The lack of significant changes in detritus storage after Year 10 can be attributed to the rate of sedimentation in the surface sediments of Tokyo Bay, which is approximately 0.5–1 cm year^{-1}. Consequently, in cases 1 and 2, ecological responses in the vicinity of the sediment–water interface, induced by the changes in bottom water DO concentrations, take approximately 20 years to propagate to a sediment depth of 10 cm, after which the benthic ecosystem reaches equilibrium. The apparent plateau in detritus storage after approximately 10 years reflects a dynamic balance between burial and remineralization, rather than a saturation of storage capacity. Organic matter is gradually transported below the 10 cm layer through sediment mixing and early diagenetic processes, leading to stabilization of vertical fluxes into and out of the upper sediment. Although the carbon in the top 10 cm has not yet reached the permanently buried layer (defined as the permanent sediment layer in the model; see Fig. 7), it actively participates in benthic carbon cycling and determines the near-future burial flux. Therefore, tracking carbon in this transitional layer is essential for assessing long-term carbon dynamics under sustained hypoxic conditions.

https://doi.org/10.5194/egusphere-2025-4822
Preprint. Discussion started: 20 October 2025

These findings provide evidence to indicate that more severe hypoxia, leading to annual anoxic conditions, would contribute to a decline in SFB due to a deficiency in oxygen. This in turn would reduce the feeding of these organisms on suspended organic matter in the pelagic system, thereby increasing the rate of pelagic detritus sedimentation (M T^{-1}). In addition, within an anaerobic environment, the rate of mineralization per unit detritus (T^{-1}) would decline, further promoting benthic detritus storage, and, as a consequence of a combination of these processes, the rate of detritus burial would increase, ultimately enhancing the carbon storage function.

Compared with previous studies, the present model provides a novel process-based formulation of microbial mineralization under varying oxygen conditions. For instance, the model by Sohma et al. (2008) distinguishes between labile and refractory organic matter with different decomposition rates, whereas it did not explicitly incorporate oxygen-dependent microbial respiration mechanisms at that stage. Similarly, Das et al. (2010) represent mineralization as an empirical function of oxygen and temperature, while providing valuable insights without explicitly considering microbial energy metabolism. In contrast, our model explicitly links the rate of organic matter decomposition to the ATP production efficiency under different redox conditions. This enables the simulation of shifts in microbial metabolic strategies e.g., from aerobic to anaerobic pathways, thereby enabling a more realistic representation of carbon mineralization and detritus accumulation under hypoxic stress. Such bioenergetic-based modeling provides deeper insights into benthic carbon cycling and is adaptable to other coastal systems experiencing seasonal hypoxia.

Although previous models applied to hypoxia-prone systems such as Chesapeake Bay (e.g., Sturdivant et al., 2013) and the Black Sea (e.g., Yakushev et al., 2007) have explored hypoxia impacts on benthic carbon cycling using empirical or static formulations, our model introduces a mechanistic coupling between microbial respiration pathways and ATP production efficiency. This enables a dynamic representation of organic matter mineralization across redox gradients, thereby advancing beyond existing empirical models in both explanatory depth and cross-system applicability.

6.3 Mechanistic analysis of benthic $CaCO_3$ dynamics

Similar to the analysis of benthic detritus, the mechanisms associated with the production and consumption of $CaCO_3$ in the benthic system were analyzed to gain an understanding of the factors contributing to changes in carbon storage function and the long-term variations in carbon storage up to sediment depths of 10 cm (t C). Figure 11 illustrates the processes involved in $CaCO_3$ production and consumption based on this analysis. Figure 12 illustrates the time-series changes in the annual average

https://doi.org/10.5194/egusphere-2025-4822
Preprint. Discussion started: 20 October 2025

rates of $CaCO_3$ production and consumption across the entire calculation domain, whereas Fig. 13 shows the differences between the hypoxic condition (Case 1) and the non-hypoxic condition (Case 2), represented as Case 1 minus Case 2.

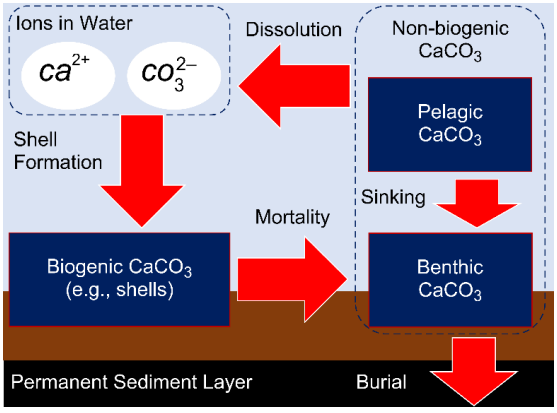

Figure 11. A conceptual diagram of the mechanisms associated with $CaCO_3$ production and consumption mechanisms in the benthic system.

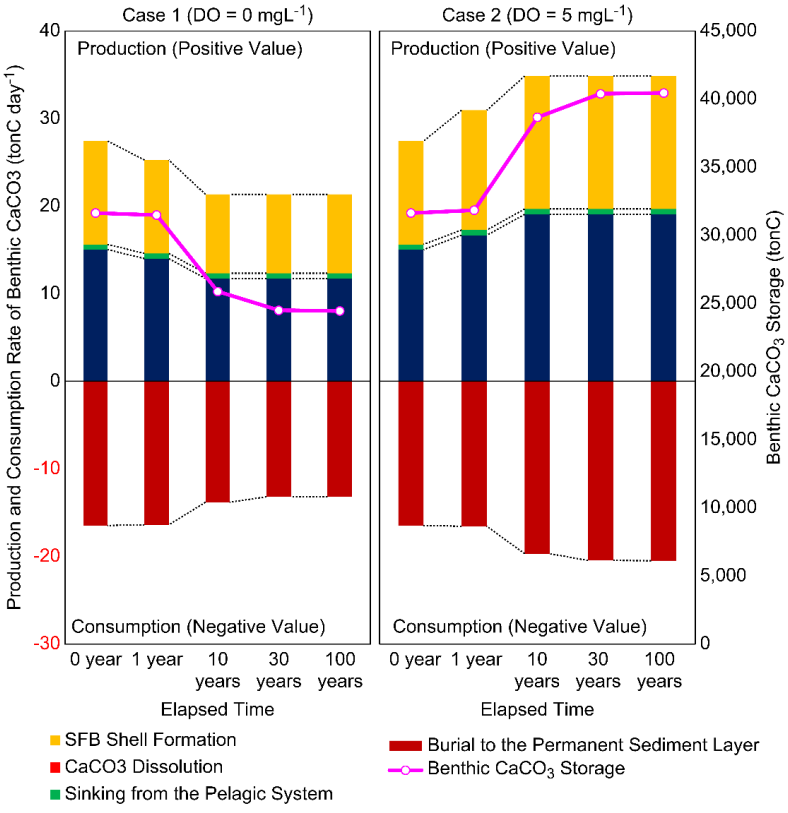

Figure 12. The rates of $CaCO_3$ production and consumption in the benthic system. Total values across the entire benthic system (728 km² × 10 cm) (positive for production and negative for consumption).

https://doi.org/10.5194/egusphere-2025-4822
Preprint. Discussion started: 20 October 2025

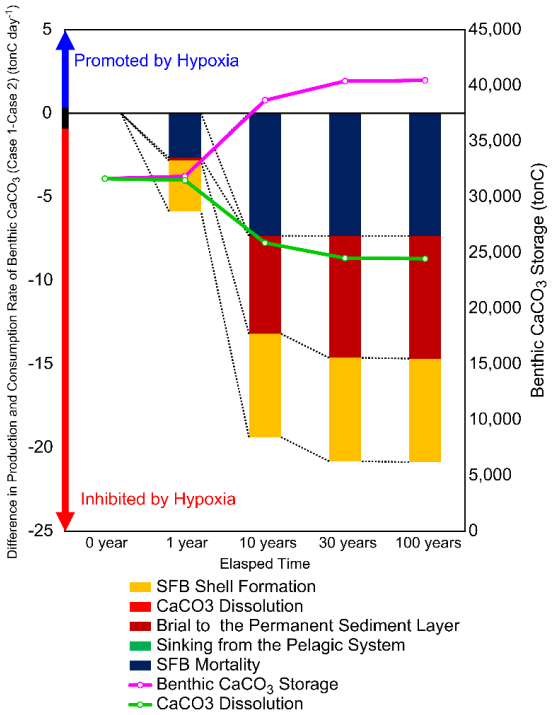

Figure 13. Differences in the rates of $CaCO_3$ production and consumption in the benthic system between Case 1 and Case 2 (Case 1 − Case 2). Annual average values are provided across the entire benthic system (728 km² × 10 cm), with positive values reflecting increases in production or consumption under specific conditions and negative values showing the converse.

As shown in Fig. 12, it is evident that the rate of benthic $CaCO_3$ production is largely influenced by SFB shell formation and the deposition of $CaCO_3$ resulting from SFB mortality, whereas the rate of $CaCO_3$ consumption is determined primarily by its burial within permanent sediment layers.

Figure 13 shows significant negative values for the rates of shell formation and $CaCO_3$ deposition due to SFB mortality [representing the rate of $CaCO_3$ input to sediments (M T^{-1})]. Compared with that in Case 2, the considerably lower biomass of SFB in Case 1 indicates that hypoxic conditions lead to a substantial reduction in shell formation and a decline in the input of shells to the sediments. Furthermore, the reductions in these rates are more pronounced in Year 10 than in Year 1, which is attributed to the fact that the biomass of SFB (M) is significantly lower after several years of hypoxic exposure, particularly after experiencing repeated hypoxic events each August.

The large negative values for burial rates (M T^{-1}) observed after Year 10 can be ascribed to the near-total extinction of SFB by Year 10 under hypoxic conditions (Case 1), whereas some SFB survived in Year 1. This decline in SFB biomass results in a reduced input of shells (M T^{-1}) to the benthic system, further diminishing the deposition and burial of $CaCO_3$.

https://doi.org/10.5194/egusphere-2025-4822
Preprint. Discussion started: 20 October 2025

These findings reveal that hypoxia-induced SFB mortality leads to reductions in shell formation ($CaCO_3$ production) and the input of shells ($CaCO_3$) to sediments, thereby resulting in corresponding reductions in the rates of $CaCO_3$ storage and burial in the benthic system.

In many previous models, shell formation and the burial of $CaCO_3$ have typically been formulated as static or empirical processes, governed by physicochemical parameters such as bottom-water oxygen concentration, sedimentation rate, and carbonate saturation state (e.g., Cartapanis et al., 2018; Dunne et al., 2012; Kanzaki et al., 2021; van Cappellen and Wang, 2002). In contrast, the present model explicitly incorporates dynamic feedback between the biomass of SFB and $CaCO_3$ fluxes – namely, shell formation and burial – enabling a more mechanistic and biologically consistent representation of benthic carbonate cycling. This biologically driven formulation enables the dynamic elucidation of the influence of seasonal or chronic hypoxia-induced variations in benthic faunal populations on carbonate cycling over decadal timescales.

By incorporating cumulative hypoxic stress into the suppression of shell formation and SFB recovery, rather than relying on instantaneous DO thresholds, the model enables more realistic projections of long-term carbonate input and burial rates. Moreover, in contrast to empirical diagenetic models that simulate sediment chemistry independently of faunal feedback, our framework explicitly links benthic biological processes with carbon storage functions.

These innovations facilitate an integrated understanding of benthic inorganic carbon dynamics, especially under conditions of seasonal or chronic hypoxia, and offer improved mechanistic fidelity compared to earlier models that do not fully resolve oxygen–biomass–carbon feedback.

7. Conclusion

In this study, we describe a novel extension of the benthic–pelagic coupled model EMAGIN-B.C. and demonstrate its application in evaluating the biogeochemical effects of hypoxia on benthic carbon storage. The extended model EMAGIN-B.C.-MR integrates two key mechanisms: (a) redox-sensitive mineralization rates linked to microbial ATP production efficiency, and (b) hypoxia-induced mortality and metabolic suppression in benthic fauna, based on DO saturation thresholds. In addition, the model explicitly couples the biomass of SFB with the production and burial fluxes of $CaCO_3$, facilitating a biologically driven simulation of carbonate cycling under changing oxygen conditions.

These model enhancements enabled us to capture the compound effects of oxygen depletion on benthic carbon dynamics, showing that detritus and $CaCO_3$ fluxes are shaped not by any single process but by the interaction of reduced microbial

https://doi.org/10.5194/egusphere-2025-4822
Preprint. Discussion started: 20 October 2025

degradation and faunal mortality. Application of EMAGIN-B.C.-MR to Tokyo Bay – a eutrophic, hypoxia-prone coastal system – revealed that declining mineralization rates, in combination with increased mortality of SFB, led to enhanced detritus storage and burial. At the same time, shell formation and carbonate deposition were suppressed, resulting in long-term reductions in $CaCO_3$ burial. These mechanisms were especially pronounced after repeated seasonal hypoxic events and revealed nonlinear, decadal-scale responses in benthic carbon storage.

By explicitly incorporating microbial energetics, DO-sensitive faunal mortality, and faunal-carbonate feedback, the model advances mechanistic understanding of the role of oxygen availability in modulating benthic carbon cycling through intertwined microbial and macrofaunal pathways. These biogeochemical insights are directly relevant for predicting the role of coastal systems in carbon budgets and for informing blue carbon management strategies under progressive deoxygenation. Moreover, the framework is not limited to Tokyo Bay but is broadly transferable to hypoxia-prone systems worldwide (e.g., Chesapeake Bay, Black Sea, Osaka Bay), thereby supporting cross-system comparisons and future climate change assessments. This transferable framework provides a basis for integrating process-based models into assessments of coastal carbon sequestration under future climate and anthropogenic pressures.

Declaration of generative AI and AI-assisted technologies in the writing process

During the preparation of this work, the authors used DeepL software to assist in identifying the most appropriate English expressions to use. After using this tool/service, the authors reviewed and edited the content as needed and take full responsibility for the content of the publication.

Data availability

Data from the study are available from the corresponding author upon reasonable request. However, any confidential or sensitive information will be omitted and cannot be shared.

https://doi.org/10.5194/egusphere-2025-4822
Preprint. Discussion started: 20 October 2025

CRediT authorship contribution statement

Akio Sohma: Conceptualization, Data curation, Funding acquisition, Investigation, Methodology, Project administration, Resources, Software, Supervision, Writing – original draft, Writing – review & editing; Kota Ishizuka: Data curation, Formal analysis, Investigation, Software, Validation, Visualization, Writing – original draft, Writing – review & editing.

Declaration of competing interests

The authors declare that they have no known competing financial interests or personal relationships that could have appeared to influence the work reported in this paper.

Acknowledgments

Part of this study represents Master's thesis research conducted by Kota Ishizuka under the supervision of Akio Sohma.

Financial support

This study was partially supported by the Environment Research and Technology Development Fund (JPMEERF24S12312) of the Environmental Restoration and Conservation Agency provided by the Ministry of the Environment of Japan, the Fisheries Agency of Japan, and JSPS KAKENHI (18K04409), all granted to A.S.

References

Alongi, D. M., Murdiyarso, D., Fourqurean, J. W., Kauffman, J. B., Hutahaean, A., Crooks, S., Lovelock, C. E., Howard, J., Herr, D., Fortes, M., Pidgeon, E., and Wagey, T.: Indonesia's blue carbon: A globally significant and vulnerable sink for seagrass and mangrove carbon, Wetlands Ecol. Manag., 24, 3–13, https://doi.org/10.1007/s11273-015-9446-y, 2016.

Andersen, F. O.: Fate of organic carbon added as diatom cells to oxic and anoxic marine sediment microcosms, Mar. Ecol. Prog. Ser., 134, 225–233, https://doi.org/10.3354/meps134225, 1996.

https://doi.org/10.5194/egusphere-2025-4822
Preprint. Discussion started: 20 October 2025

Anderson, L. G., Hall, P. O. J., Iverfeldt, A., Rutgers van der Loejf, M. M., Sundby, B., and Westerlund, S. F. G.: Benthic respiration measured by total carbonate production, Limnol. Oceanogr., 31, 319–329, https://doi.org/10.4319/lo.1986.31.2.0319, 1986.

Archer, D. and Brovkin, V.: The millennial atmospheric lifetime of anthropogenic CO_2, Clim. Change, 90, 283–297, https://doi.org/10.1007/s10584-008-9413-1, 2008.

Aumont, O., Maier-Reimer, E., Blain, S., and Monfray, P.: An ecosystem model of the global ocean including Fe, Si, P colimitations, Glob. Biogeochem. Cycles, 17, 1060, https://doi.org/10.1029/2001GB001745, 2003.

Bailey, J. E. and Ollis, D. F.: Biochemical engineering fundamentals, McGraw-Hill, New York, 1986.

Bastviken, D., Olsson, M., and Tranvik, L.: Simultaneous measurements of organic carbon mineralization and bacterial production in oxic and anoxic lake sediments, Microb. Ecol., 46, 73–82, https://doi.org/10.1007/s00248-002-1061-9, 2003.

Benner, R., Maccubbin, A. E., and Hodson, R. E.: Anaerobic biodegradation of the lignin and polysaccharide components of lignocellulose and synthetic lignin by sediment microflora, Appl. Environ. Microbiol., 47, 998–1004, https://doi.org/10.1128/aem.47.5.998-1004.1984, 1984.

Blackburn, T. H.: Accumulation and regeneration: Processes at the benthic boundary layer, in: Ocean Margin Processes in Global Change, edited by: Mantoura, R. F. C., Martin, J. M., Wollast, R., John Wiley & Sons Inc., London, 181–195, 1991.

Breitburg, D., Levin, L. A., Oschlies, A., Grégoire, M., Chavez, F. P., Conley, D. J., Garçon, V., Gilbert, D., Gutiérrez, D., Isensee, K., Jacinto, G. S., Limburg, K. E., Montes, I., Naqvi, S. W. A., Pitcher, G. C., Rabalais, N. N., Roman, M. R., Rose, K. A., Seibel, B. A., Telszewski, M., Yasuhara, M., and Zhang, J.: Declining oxygen in the global ocean and coastal waters, Science, 359, eaam7240, https://doi.org/10.1126/science.aam7240, 2018.

Burdige, D. J.: Preservation of organic matter in marine sediments: Controls, mechanisms, and an imbalance in sediment organic carbon budgets?, Chem. Rev., 107, 467–485, https://doi.org/10.1021/cr050347q, 2007.

Butenschön, M., Clark, J., Aldridge, J. N., Allen, J. I., Artioli, Y., Blackford, J., Bruggeman, J., Cazenave, P., Ciavatta, S., Kay, S., Lessin, G., van Leeuwen, S., van der Molen, J., de Mora, L., Polimene, L., Sailley, S., Stephens, N., and Torres, R.: ERSEM 15.06: A generic model for marine biogeochemistry and the ecosystem dynamics of the lower trophic levels, Geosci. Model Dev., 9, 1293–1339, https://doi.org/10.5194/gmd-9-1293-2016, 2016.

https://doi.org/10.5194/egusphere-2025-4822
Preprint. Discussion started: 20 October 2025

Canfield, D. E., Kristensen, E., and Thamdrup, B.: Thermodynamics and microbial metabolism, Adv. Mar. Biol., 48, 65–94. https://doi.org/10.1016/S0065-2881(05)48003-7, 2005.

Canfield, D. E.: Factors influencing organic carbon preservation in marine sediments, Chem. Geol., 114, 315–329. https://doi.org/10.1016/0009-2541(94)90061-2, 1994.

Canfield, D. E.: Organic matter oxidation in marine sediments. Interactions of C, N, P, and S biogeochemical cycles and global change, Springer, Berlin, 333–363, 1993.

Canfield, D. E.: Sulfate reduction and oxic respiration in marine sediments: Implications for organic carbon preservation in euxinic environments, Deep Sea Res. A, 36, 121–138, https://doi.org/10.1016/0198-0149(89)90022-8, 1989.

Carey, C. C., Doubek, J. P., McClure, R. P., and Hanson, P. C.: Oxygen dynamics control the burial of organic carbon in a eutrophic reservoir, Limnol. Oceanogr. Lett., 3, 293–301, https://doi.org/10.1002/lol2.10057, 2018.

Cartapanis, O., Galbraith, E. D., Bianchi, D., and Jaccard, S. L.: Carbon burial in deep-sea sediment and implications for oceanic inventories of carbon and alkalinity over the last glacial cycle, Clim. Past, 14, 1819–1850, https://doi.org/10.5194/cp-14-1819-2018, 2018.

Cerco, C. F., Noel, M. R., and Kim, S. C.: Three-dimensional management model for Lake Washington, part II: Eutrophication modeling and skill assessment, Lake Reservoir Manag., 22, 115–131, https://doi.org/10.1080/07438140609353889, 2006.

Chen, C.-T. A., Huang, T.-H., Chen, Y.-C., Bai, Y., He, X., and Kang, Y.: Air-sea exchanges of CO_2 in the world's coastal seas, Biogeosciences, 10, 6509–6544, https://doi.org/10.5194/bg-10-6509-2013, 2013.

Chmura, G. L., Anisfeld, S. C., Cahoon, D. R., and Lynch, J. C.: Global carbon sequestration in tidal, saline wetland soils, Global Biogeochem. Cycles, 17, https://doi.org/10.1029/2002GB001917, 2003.

Cowie, G. L., Hedges, J. I., Prahl, F. G., and de Lange, G. J.: Elemental and major biochemical changes across an oxidation front in a relict turbidite: An oxygen effect, Geochim. Cosmochim. Acta, 59, 33–46, https://doi.org/10.1016/0016-7037(94)00329-K, 1995.

Das, A., Justić, D., and Swenson, E.: Modeling estuarine-shelf exchanges in a deltaic estuary: Implications for coastal carbon budgets and hypoxia, Ecol. Modell., 221, 978–985, https://doi.org/10.1016/j.ecolmodel.2009.01.023, 2010.

Diaz, R. J. and Rosenberg, R.: Marine benthic hypoxia: A review of its ecological effects and the behavioural responses of benthic macrofauna, Oceanogr. Mar. Biol. Annu. Rev., 33, 245–303, 1995.

https://doi.org/10.5194/egusphere-2025-4822
Preprint. Discussion started: 20 October 2025

Diaz, R. J.: Overview of hypoxia around the world, J. Environ. Qual., 30, 275–281, https://doi.org/10.2134/jeq2001.302275x, 2001.

Donato, D. C., Kauffman, J. B., Murdiyarso, D., Kurnianto, S., Stidham, M., and Kanninen, M.: Mangroves among the most carbon-rich forests in the tropics, Nat. Geosci., 4, 293–297, https://doi.org/10.1038/ngeo1123, 2011.

Dunne, J. P., Hales, B., and Toggweiler, J. R.: Global calcite cycling constrained by sediment preservation controls, Glob. Biogeochem. Cycles, 26, GB3023, https://doi.org/10.1029/2010GB003935, 2012.

Emerson, S. and Hedges, J. I.: Processes controlling the organic carbon content of open ocean sediments, Paleoceanography, 3, 621–634, https://doi.org/10.1029/PA003i005p00621, 1988.

Falkowski, P., Scholes, R. J., Boyle, E., Canadell, J., Canfield, D., Elser, J., Gruber, N., Hibbard, K., Högberg, P., Linder, S., Mackenzie, F. T., Moore, B., 3rd, Pedersen, T., Rosenthal, Y., Seitzinger, S., Smetacek, V., and Steffen, W.: The global carbon cycle: A test of our knowledge of earth as a system, Science, 290, 291–296, https://doi.org/10.1126/science.290.5490.291, 2000.

Fallon, R. D. and Brock, T. D.: Decomposition of blue-green algal (cyanobacterial) blooms in Lake Mendota, Wisconsin, Appl. Environ. Microbiol., 37, 820–830, https://doi.org/10.1128/aem.37.5.820-830.1979, 1979.

Fenchel, T. and Finlay, B. J.: Ecology and evolution in anoxic worlds, Oxford University Press, Oxford, https://doi.org/10.1093/oso/9780198548386.001.0001, 1995.

Fennel, K., Hetland, R., Feng, Y., and DiMarco, S.: A coupled physical-biological model of the northern Gulf of Mexico shelf: Model description, validation and analysis of phytoplankton variability, Biogeosciences, 8, 1881–1899, https://doi.org/10.5194/bg-8-1881-2011, 2011.

Flynn, K. J.: Ecological modelling in a sea of variable stoichiometry: Dysfunctionality and the legacy of Redfield and Monod, Prog. Oceanogr., 84, 52–65, https://doi.org/10.1016/j.pocean.2009.09.006, 2010.

Fourqurean, J. W., Duarte, C. M., Kennedy, H., Marbà, N., Holmer, M., Mateo, M. A., Apostolaki, E. T., Kendrick, G. A., Krause-Jensen, D., McGlathery, K. J., and Serrano, O.: Seagrass ecosystems as a globally significant carbon stock, Nat. Geosci., 5, 505–509, https://doi.org/10.1038/ngeo1477, 2012.

Frankignoulle, M., Abril, G., Borges, A., Bourge, I., Canon, C., Delille, B., Libert, E., and Theate, J. M.: Carbon dioxide emission from European estuaries, Science, 282, 434–436, https://doi.org/10.1126/science.282.5388.434, 1998.

https://doi.org/10.5194/egusphere-2025-4822
Preprint. Discussion started: 20 October 2025

Garcia, H. E. and Gordon, L. I.: Oxygen solubility in seawater: Better fitting equations, Limnol. Oceanogr., 37, 1307–1312, https://doi.org/10.4319/lo.1992.37.6.1307, 1992.

Gray, J. S., Wu, R. S. S., and Or, Y. Y.: Effects of hypoxia and organic enrichment on the coastal marine environment, Mar. Ecol. Prog. Ser., 238, 249–279, https://doi.org/10.3354/meps238249, 2002.

Hansen, L. S. and Blackburn, T. H.: Aerobic and anaerobic mineralization of organic material in marine sediment microcosms, Mar. Ecol. Prog. Ser., 75, 283–291, https://doi.org/10.3354/meps075283, 1991.

Hanyu, K.: Investigation into the beginning of hypoxia expansion across the inner part of Ise Bay, Bol. Mie Prefect. Fish. Res. Inst., 26, 53–66, 2020 (in Japanese).

Hartnett, H. E., Keil, R. G., Hedges, J. I., and Devol, A. H.: Influence of oxygen exposure time on organic carbon preservation in continental margin sediments, Nature, 391, 572–575, https://doi.org/10.1038/35351, 1998.

Hedges, J. I. and Keil, R. G.: Sedimentary organic matter preservation: An assessment and speculative synthesis, Mar. Chem., 49, 81–115, https://doi.org/10.1016/0304-4203(95)00008-F, 1995.

Hedges, J. I.: Sedimentary organic matter preservation; a test for selective degradation under oxic conditions, Am. J. Sci., 299, 529–555, https://doi.org/10.2475/ajs.299.7-9.529, 1999.

Hollander, D. J., McKenzie, J. A., and Haven, H. L.: A 200 year sedimentary record of progressive eutrophication in Lake Greifen (Switzerland): Implications for the origin of organic-carbon-rich sediments, Geology, 20, 825–828, https://doi.org/10.1130/0091-7613(1992)020<0825:AYSROP>2.3.CO;2, 1992.

Hulthe, G., Hulth, S., and Hall, P. O. J.: Effect of oxygen on degradation rate of refractory and labile organic matter in continental margin sediments, Geochim. Cosmochim. Acta, 62, 1319–1328, https://doi.org/10.1016/S0016-7037(98)00044-1, 1998.

Ingall, E. D., Bustin, R. M., and Van Cappellen, P.: Influence of water column anoxia on the burial and preservation of carbon and phosphorus in marine shales, Geochim. Cosmochim. Acta, 57, 303–316, https://doi.org/10.1016/0016-7037(93)90433-W, 1993.

IPCC: The physical science basis, Contrib. Working Group I to the fourth assessment report of the Intergovernmental Panel on Climate Change (IPCC) Solomon, in: Climate Change, edited by: Qin, S., D., Manning, M., Chen, Z., Marquis, M., Averyt, K. B., Tignor, M., and Miller, H. L., Cambridge University Press, Cambridge, UK, 996, 2007.

https://doi.org/10.5194/egusphere-2025-4822
Preprint. Discussion started: 20 October 2025

IPCC: The physical science basis: Working Group I contribution to the sixth assessment report of the Intergovernmental Panel on Climate Change, edited by: Masson-Delmotte, V., Zhai, P., Pirani, A., Connors, S. L., Péan, C., Berger, S., Caud, N., Chen, Y., Goldfarb, L., Gomis, M. I., Huang, M., Leitzell, K., Lonnoy, E., Matthews, J. B. R., Maycock, T. K., Waterfield, T., Yelekçi, O., Yu, R., and Zhou, B., Cambridge University Press, UK, 2391, https://doi.org/10.1017/9781009157896, 2023.

Ishii, M. and Ohata, S.: Variations in water quality and hypoxic water mass in Tokyo Bay. Bol. Coast. Oceanogr., 48, 37–44, 2010 (in Japanese).

Isidorova, A., Mendonça, R., and Sobek, S.: Reduced mineralization of terrestrial OC in anoxic sediment suggests enhanced burial efficiency in reservoirs compared to other depositional environments, J. Geophys. Res. Biogeosci., 124, 678–688, https://doi.org/10.1029/2018JG004823, 2019.

Jin, Q.: Energy conservation of anaerobic respiration, Am. J. Sci., 312, 573–628, https://doi.org/10.2475/06.2012.01, 2012.

Kanzaki, Y., Hülse, D., Kirtland Turner, S., and Ridgwell, A.: A model for marine sedimentary carbonate diagenesis and paleoclimate proxy signal tracking: IMP v1.0, Geosci. Model Dev., 14, 5999–6023, https://doi.org/10.5194/gmd-14-5999-2021, 2021.

Katsev, S. and Crowe, S. A.: Organic carbon burial efficiencies in sediments: The power law of mineralization revisited, Geology, 43, 607–610, https://doi.org/10.1130/G36626.1, 2015.

Kristensen, E. and Holmer, M.: Decomposition of plant materials in marine sediment exposed to different electron acceptors (O_2, NO_3^-, and SO_4^{2-}), with emphasis on substrate origin, degradation kinetics, and the role of bioturbation, Geochim. Cosmochim. Acta, 65, 419–433, https://doi.org/10.1016/S0016-7037(00)00532-9, 2001.

Kubo, A. and Kanda, J.: Seasonal variations and sources of sedimentary organic carbon in Tokyo Bay, Mar. Pollut. Bull., 114, 637–643, https://doi.org/10.1016/j.marpolbul.2016.10.030, 2017.

Kuwae, T., Kanda, J., Kubo, A., Nakajima, F., Ogawa, H., Sohma, A., and Suzumura, M.: Blue carbon in human-dominated estuarine and shallow coastal systems, Ambio, 45, 290–301, https://doi.org/10.1007/s13280-015-0725-x, 2016.

LaRowe, D. E. and Van Cappellen, P.: Degradation of natural organic matter: A thermodynamic analysis, Geochim. Cosmochim. Acta, 75, 2030–2042, https://doi.org/10.1016/j.gca.2011.01.020, 2011.

https://doi.org/10.5194/egusphere-2025-4822
Preprint. Discussion started: 20 October 2025

McLeod, E., Chmura, G. L., Bouillon, S., Salm, R., Björk, M., Duarte, C. M., Lovelock, C. E., Schlesinger, W. H., and Silliman, B. R.: A blueprint for blue carbon: Toward an improved understanding of the role of vegetated coastal habitats in sequestering CO_2, Front. Ecol. Environ., 9, 552–560, https://doi.org/10.1890/110004, 2011.

Meire, L. K. E. R., Soetaert, K. E. R., and Meysman, F. J. R.: Impact of global change on coastal oxygen dynamics and risk of hypoxia, Biogeosciences, 10, 2633–2653, https://doi.org/10.5194/bg-10-2633-2013, 2013.

Murdiyarso, D., Purbopuspito, J., Kauffman, J. B., Warren, M. W., Sasmito, S. D., Donato, D. C., Manuri, S., Krisnawati, H., Taberima, S., and Kurnianto, S.: The potential of Indonesian mangrove forests for global climate change mitigation, Nat. Clim. Change, 5, 1089–1092, https://doi.org/10.1038/nclimate2734, 2015.

Nagao, K., Hibino, T., and Matsumoto, H.: Analysis of organic matter fluctuations and identification of nutrient generation forms in Hiroshima Bay, Coast. Eng. J., 52, 916–920, 2005 (in Japanese).

Nellemann, C., Corcoran, E., Duarte, C. M., Valdes, L., De Young, C., Fonseca, L., and Grimsditch, G.: Blue carbon: The role of healthy oceans in binding carbon: A rapid response assessment. UN Environmental Program/Earthprint, 78, 2009.

Nguyen, R. T. and Harvey, H. R.: Protein and amino acid cycling during phytoplankton decomposition in oxic and anoxic waters, Org. Geochem., 27, 115–128, https://doi.org/10.1016/S0146-6380(97)00076-4, 1997.

Okubo, K., Ono, T., Nakano, K., Ushiro, M., and Fujiwara, T.: Variability and duration of hypoxia in Osaka Bay, J. Jpn Soc. Water Environ. (Survey Paper), 39, 233–240, https://doi.org/10.2965/jswe.39.233, 2016 (in Japanese).

Paropkari, A. L., Babu, C. P., and Mascarenhas, A.: New evidence for enhanced preservation of organic carbon in contact with the oxygen minimum zone on the western continental slope of India, Mar. Geol., 111, 7–13, https://doi.org/10.1016/0025-3227(93)90185-X, 1993.

Payne, W. J.: Energy yields and growth of heterotrophs, Annu. Rev. Microbiol., 24, 17–52, https://doi.org/10.1146/annurev.mi.24.100170.000313, 1970.

Rabalais, N. N., Turner, R. E., Díaz, R. J., and Justić, D.: Global change and eutrophication of coastal waters, ICES J. Mar. Sci., 66, 1528–1537, https://doi.org/10.1093/icesjms/fsp047, 2009.

Reed, D. C., Slomp, C. P., and Gustafsson, B. G.: Sedimentary phosphorus dynamics and the evolution of bottom-water hypoxia: A coupled benthic–pelagic model of a coastal system, Limnol. Oceanogr., 56, 1075–1092, https://doi.org/10.4319/lo.2011.56.3.1075, 2011.

https://doi.org/10.5194/egusphere-2025-4822
Preprint. Discussion started: 20 October 2025

Rodger Harvey, H., Tuttle, J. H., and Tyler Bell, J.: Kinetics of phytoplankton decay during simulated sedimentation: Changes in biochemical composition and microbial activity under oxic and anoxic conditions, Geochim. Cosmochim. Acta, 59, 3367–3377, https://doi.org/10.1016/0016-7037(95)00217-N, 1995.

Russell, J. B. and Cook, G. M.: Energetics of bacterial growth: Balance of anabolic and catabolic reactions, Microbiol. Rev., 59, 48–62, https://doi.org/10.1128/mr.59.1.48-62.1995, 1995.

Sasaki, N., Tabeta, S., and Kitazawa, D.: Long-term continuous simulation of the ecosystem in Tokyo Bay considering changes of load and topography, J. Coast. Zone Stud., 21, 27–28, 2009 (in Japanese).

Shimo, S., Akimoto, Y., and Takahama, H.: Review of the water quality effects on marine organisms tolerance: A review, Bol. Mar. Ecol. Res. Inst., 6, 1–159, 2004 (in Japanese).

Sobek, S., Durisch-Kaiser, E., Zurbrügg, R., Wongfun, N., Wessels, M., Pasche, N., and Wehrli, B.: Organic carbon burial efficiency in lake sediments controlled by oxygen exposure time and sediment source, Limnol. Oceanogr., 54, 2243–2254, https://doi.org/10.4319/lo.2009.54.6.2243, 2009.

Soetaert, K. and Middelburg, J. J.: Modeling eutrophication and oligotrophication of shallow-water marine systems: The importance of sediments under stratified and well-mixed conditions, Hydrobiologia, 629, 239–254, https://doi.org/10.1007/s10750-009-9777-x, 2009.

Soetaert, K., Herman, P. M. J., and Middelburg, J. J.: A model of early diagenetic processes from the shelf to abyssal depths, Geochim. Cosmochim. Acta, 60, 1019–1040, https://doi.org/10.1016/0016-7037(96)00013-0, 1996.

Sohma, A., Sekiguchi, Y., Kuwae, T., and Nakamura, Y.: A benthic–pelagic coupled ecosystem model to estimate the hypoxic estuary including tidal flat—Model description and validation of seasonal/daily dynamics, Ecol. Modell., 215, 10–39, https://doi.org/10.1016/j.ecolmodel.2008.02.027, 2008.

Sohma, A., Shibuki, H., Nakajima, F., Kubo, A., and Kuwae, T.: Modeling a coastal ecosystem to estimate climate change mitigation and a model demonstration in Tokyo Bay, Ecol. Modell., 384, 261–289, https://doi.org/10.1016/j.ecolmodel.2018.04.019, 2018.

Stock, C. A., Dunne, J. P., and John, J. G.: Global-scale carbon and energy flows through the marine planktonic food web: An analysis with a coupled physical–biological model, Prog. Oceanogr., 120, 1–28, https://doi.org/10.1016/j.pocean.2013.07.001, 2014.

https://doi.org/10.5194/egusphere-2025-4822
Preprint. Discussion started: 20 October 2025

Sturdivant, S. K., Brush, M. J., and Díaz, R. J.: Modeling the effect of hypoxia on macrobenthos production in the lower Rappahannock River, Chesapeake Bay, USA, PLOS One, 8, e84140, https://doi.org/10.1371/journal.pone.0084140, 2013.

Sun, M. Y., Lee, C., and Aller, R. C.: Laboratory studies of oxic and anoxic degradation of chlorophyll-a in Long Island sediments, Geochim. Cosmochim. Acta, 57, 147–157, https://doi.org/10.1016/0016-7037(93)90475-C, 1993.

Sun, M. Y., Wakeham, S. G., and Lee, C.: Rates and mechanisms of fatty acid degradation in oxic and anoxic coastal marine sediments of Long Island Sound, New York, USA, Geochim. Cosmochim. Acta, 61, 341–355, https://doi.org/10.1016/S0016-7037(96)00315-8, 1997.

van Cappellen, P. and Wang, Y.: Cycling of iron and manganese in surface sediments: A general theory for the coupled transport and reaction of carbon, oxygen, nitrogen, sulfur, iron, and manganese, Am. J. Sci., 302, 729–775, https://doi.org/10.2475/ajs.296.3.197, 2002.

Wild-Allen, K., Herzfeld, M., Thompson, P. A., Rosebrock, U., Parslow, J., and Volkman, J. K.: Applied coastal biogeochemical modelling to quantify the environmental impact of fish farm nutrients and inform managers, J. Mar. Syst., 81, 134–147, https://doi.org/10.1016/j.jmarsys.2009.12.013, 2010.

Wilson, T. R. S., Thomson, J., Colley, S., Hydes, D. J., Higgs, N. C., and Sørensen, J.: Early organic diagenesis: The significance of progressive subsurface oxidation fronts in pelagic sediments, Geochim. Cosmochim. Acta, 49, 811–822, https://doi.org/10.1016/0016-7037(85)90174-7, 1985.

Yakushev, E. V., Pollehne, F., Jost, G., Kuznetsov, I., Schneider, B., Umlauf, L.: Analysis of the water column oxic/anoxic interface in the Black and Baltic seas with a numerical model, Mar. Chem., 107, 388–410, https://doi.org/10.1016/j.marchem.2007.06.003, 2007.

Yakushev, E. V., Protsenko, E. A., Bruggeman, J., Wallhead, P., Pakhomova, S. V., Yakubov, S. Kh., Bellerby, R. G. J., and Couture, R.-M.: Bottom RedOx model (Brom v.1.1): A coupled benthic–pelagic model for simulation of water and sediment biogeochemistry, Geosci. Model Dev., 10, 453–482, https://doi.org/10.5194/gmd-10-453-2017, 2017.

Yool, A., Popova, E. E., and Anderson, T. R.: MEDUSA-2.0: An intermediate complexity biogeochemical model of the marine carbon cycle for climate change and ocean acidification studies, Geosci. Model Dev., 6, 1767–1811, https://doi.org/10.5194/gmd-6-1767-2013, 2013.

https://doi.org/10.5194/egusphere-2025-4822
Preprint. Discussion started: 20 October 2025

Zehnder, A. J. B. and Stumm, W.: Geochemistry and biogeochemistry of anaerobic habitats, in: Biology of anaerobic microorganisms, edited by: Zehnder, A. J. B., John Wiley & Sons, New York, 1–38, 1988.

Zehnder, A. J. B. and Svensson, B. H.: Life without oxygen: What can and what cannot?, Experientia, 42, 1197–1205, https://doi.org/10.1007/BF01946391, 1986.

Zsolnay, A.: Diagenesis as a function of redox conditions in nature: A comparative survey of certain organic and inorganic compounds in a oxic and anoxic Baltic Basin, Kieler Meeresforschungen, 27, 135–165, 1971.